

## **Morphological Properties and Raman Spectroscopy of ZnO Nanorods**

*A. K. Bhunia<sup>1,2</sup>, P. K. Jha<sup>3</sup>, D. Rout<sup>4</sup> and S. Saha<sup>1</sup>*

<sup>1</sup>Department of Physics and Technophysics, Vidyasagar University  
Midnapore -721102, India

<sup>2</sup>Department of Physics, Government General Degree College at Gopiballavpur-II  
Beliaberah, Paschim Medinipur-721517, India

<sup>3</sup>RISUG R & D and Allied Laboratory, School of Medical Sciences & Technology  
Indian Institute of Technology Kharagpur, Kharagpur-721305, India

<sup>4</sup>Department of Chemistry, Jhargram Raj College, Paschim Medinipur-721507, India  
Email: [amitphysics87@gmail.com](mailto:amitphysics87@gmail.com)/[sahaphys.vu@gmail.com](mailto:sahaphys.vu@gmail.com)

*Received 2 November 2016; accepted 30 November 2016*

### **ABSTRACT**

The morphology of the chemically synthesized ZnO nanocrystals is observed by FESEM images, which confirms the formation of ZnO nanorods (ZnO NRs). The estimated band gap from the UV-VIS absorption spectra along with the diameter of the nanorods from FESEM showed confinement of the nanocrystals. The phonon scattering in the Raman spectra dispersed around the center of the Brillouin zone according to the uncertainty principle. The Raman spectrum showed a strong E<sub>2</sub> mode peak at nearly 435 cm<sup>-1</sup>, which confirms the wurtzite structure of zinc oxide nanorods. The photoluminescence spectrum of pure ZnO NRs showed a strong emission peak at 376 nm due to band-to-band transition. The peak positioned between A1 (LO) and E1 (LO) optical phonon mode in Raman spectroscopy correlate the emission spectra for the formation of the oxygen deficiency in the ZnO NRs.

**Keywords:** ZnO nanocrystals, FESEM, Raman spectroscopy, photoluminescence, band gap.

### **1. Introduction**

Zinc Oxide (ZnO) is very well known direct wide band gap and multifunctional semiconductor having excellent size dependent tunable optical property from blue to ultraviolet bands [1-3]. Due to large direct band gap ZnO being used in many optoelectronic devices [4] like short wavelength light-emitting, UV lasing, and It also exhibits other interesting properties, like magnetic properties, piezoelectricity, photovoltaic devices and optical solar cells , gas sensing. ZnO has high chemical and thermal stability and is not easily oxidized in the atmosphere. ZnO based semiconductor optoelectronic devices, including UV detectors, light-emitting diodes (LEDs). And semiconductor laser diodes (LDs), are widely used in optical display and storage, optical communication network, conversion, and optical detection. The key technology for ZnO-based optoelectronic devices is the fabrication of high quality ZnO materials and ZnO

thin films. The various properties of ZnO nanocrystals depend on the morphology and Size of the nanostructures. Various fabrication methods, such as physical and chemical-vapor deposition, pulsed-laser deposition, hydrothermal growth have already appeared in the literature to synthesized various types of ZnO nanostructures. Some of the above-mentioned methods have some drawbacks. Used precursors are unstable causing environmental hazards and require very high temperature, low pressure, control rate of carrier flow and many more. These methods are not cost effective also. We focused the fabrication of ZnO nanorods by a simple and cost-effective wet-chemical method. We next investigated their Morphological properties by using FESEM images. We focused our study to better understand the optical properties for ZnO nanocrystals for various optoelectronic applications. We analyse the optical properties of ZnO nanorods by using and Raman Spectroscopy and emission spectroscopy.

## 2. Experimental

All the chemicals used in this synthesis process were of analytical grade (Merck-99.99%) and used as supplied without any further purification. The details of the synthesis process has been discussed in our previous published protocol [5]. In a typical synthesis process, 0.25M of Zinc Nitrate (Hexahydrate) was first dissolved in water and kept as stock solution. 0.25M NaOH solution was added drop wise into the stock solution. The mechanical stirring was continued for 4 h. The pH of the solution was adjusting nearly 10. At the end of the reaction the white precipitate deposited at the bottom of the flux was collected, filtered, washed several times by de-ionized water and dried at 200<sup>o</sup>C for further characterizations. Scanning electron microscope (SEM) images were recorded in a Zeiss SEM operating at 5 kV. Room temperature photoluminescence (PL) data were recorded in a PERKIN ELMER LS-55 spectrometer using Xenon lamp as a source. Optical absorption measurements were carried out by using Shimadzu-Pharmaspec-1700 UV-VIS in the range 200–900 nm

## 3. Results and discussions

### 3.1. Field-emission scanning electron microscopy (FESEM)

In FESEM microscope the electrons are liberated by a field emission source then they are accelerated in a high electric field gradient. Within the high vacuum column these primary electrons are focused and deflected by electronic lenses to produce a narrow scan beam that bombards the nanomaterials. As a result secondary electrons are emitted from each spot on the material. The angle and velocity of these electrons (secondary) relates to the surface structure of the object. The secondary electrons are attracted by the Corona and strike the fluorescing mirror. The fluorescing mirror produces photons. It is used to visualize very small (in the order of nm or micro meter) topographic details on the surface or entire or fractioned objects [6]. The morphology of the fabricated ZnO nanorods was observed in a ZEISS Field emission scanning electron microscope (FESEM) operated at 5 kV. Typical FESEM images (scale 200 nm) of the deposited material under different magnification are shown in Fig. 1(a),(b),(c),(d). The formation and well aligned of ZnO rods are clear from FESEM images (Fig. 1(a),(b), (c)).The clear regions are marked by circles. Different sizes nanorods are observed from the FESEM images. The rods are confined (so called within 100nm) along diameter. The arrow sign in the figure 1(d) represent one nanorod with length  $\approx$ 400 nm.

## Morphological properties and Raman Spectroscopy of ZnO Nanorods

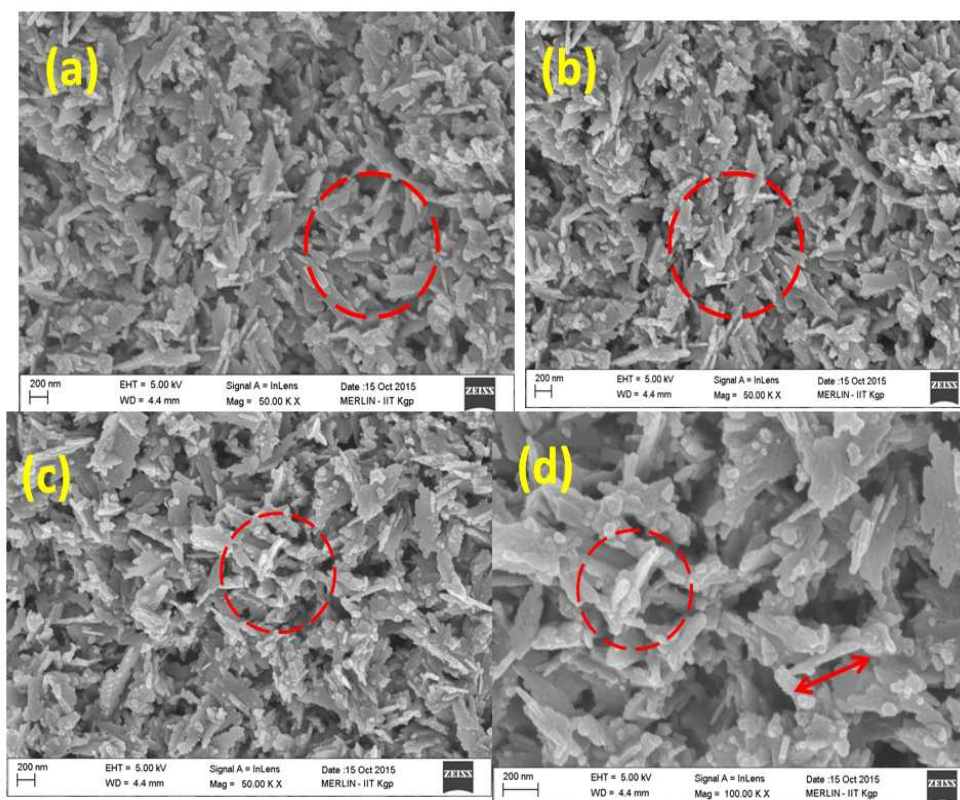


**Figure 1.** (a),(b),(c),(d) FESEM images of the ZnO nanorods

### 3.2. Raman spectroscopy

Raman scattering measures frequency shift ( $\Delta\omega = \omega_{\text{phonon}}$ ) which is the differences between incident light frequency ( $\omega_{\text{inc}}$ ) and scattered light frequency ( $\omega_{\text{scat}}$ ). Here,  $\omega_{\text{phonon}}$  is called optical phonon mode vibration. When  $\omega_{\text{phonon}}$  is an acoustic phonon, the process is called Brillouin scattering. The optical mode corresponding to high frequency lattice vibration and the acoustic mode conforms to lattice vibrations at much lower frequencies:  $\omega_{\text{acous}} \ll \omega_{\text{opt}}$ . The scattering frequency has the value  $\omega_{\text{scat}} = \omega_{\text{inc}} \pm \omega_{\text{phonon}}$  where lower frequency corresponds to a Stokes line, and the higher frequency corresponds an anti-Stokes line. These two types of scattering that entail a change in frequency of the emitted phonon are called inelastic. When there is no frequency shift (i.e.  $\Delta\omega = 0$ ), then the scattering is the elastic Rayleigh type that takes place in X-ray diffraction. Raman spectroscopy is used to studies of the vibrational properties of ZnO nanocrystals [7]. Here we describe Raman spectra from ZnO nanorods. We chemically synthesized the ZnO nanocrystals. Chemical growth of such ZnO nanostructure materials usually involves the formation of large amount of surface defects in the nanocrystals. Thus, the Raman spectra of these chemically grown ZnO nanomaterials are red shifted and broadened due to the relaxation of the selection rule for the conservation of crystal momentum (q-vector) within the finite size of the ZnO nanocrystals. According to Heisenberg uncertainty principal the phonon uncertainty is  $\Delta q \sim 1/d$ , where  $d$  is the dimension of the nanocrystal.

Also the phonon scattering in this case are no longer limited to the Brillouin zone centre but dispersed around the centre of the Brillouin zone. The crystal structure of ZnO is hexagonal with space group  $C_{6v}^4$ . Group theory shows that the Raman-active modes for ZnO crystals are  $A_1 + 2E_2 + E_1$ . The polar modes  $A_1$  and  $E_1$  can split into TO and LO modes, where TO is the transverse optical modes and LO is the longitudinal optical modes. The  $E_2$  mode is nonpolar and it composed of two modes with a low and high frequency. In our investigative of ZnO nanorods (Figure 2) shows the Prominent vibration peaks at 327, 380, 435, and 579  $cm^{-1}$ . The maximum intensity arises at 435  $cm^{-1}$  corresponding to  $E_2$  (high). The spectrum shows sharp and strong  $E_2$  mode peak at nearly 435  $cm^{-1}$ , which confirms wurtzite structure of zinc oxide nanorods [8]. The symmetry shows that peak broadens and shifts (at 435  $cm^{-1}$ ) to lower frequencies/higher wavelength compare to bulk ZnO indication of quantum confinement of the ZnO crystals [9]. The peak at 579  $cm^{-1}$ , situated between  $A_1$  (LO) and  $E_1$  (LO) optical phonon mode, arises due to the oxygen imperfection [10] This result is well agreement with the PL emission peak at 486 nm which is due to existence of oxygen deficiency. The nonpolar  $E_2$  mode is noticed at 435  $cm^{-1}$  [11]. The peak at 380  $cm^{-1}$  is assigned to  $A_1$  transverse mode and appears due to the anisotropic nature in the force constant. The  $A_1$  transverse mode has a different frequency from  $E_1$  transverse phonon mode. The peak at 327  $cm^{-1}$  is due to  $A_1$  symmetry of the modes arises due to acoustic Overtone process [7, 12].

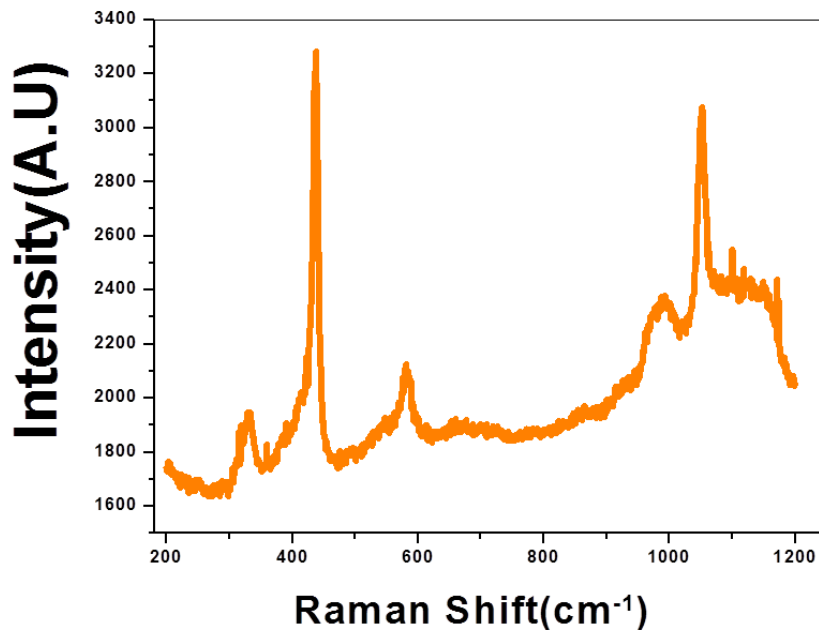


Figure 2. Raman spectra of ZnO nanorods

### 3.3. Emission spectroscopy

Figure 3 shows the emission spectra of ZnO NRs. The ZnO NRs shows a strong unique emission band around 376 nm which is in the ultraviolet emission band. A blue emission band is at 453 nm could be detected [26]. The blue emission is due to the purity of the ZnO NRs. There are different types of defects arising in ZnO nanocrystals. These are: Zn-vacancy, O-vacancy, Zn-interstitial, O-interstitial, Zn-antisite, and O-antisite. Also, there

## Morphological properties and Raman Spectroscopy of ZnO Nanorods

exists another blue emission band in the centre at 486 nm ( 2.55 eV), attributed to the presence of some defects which would be resulted from oxygen vacancies and interstitial zinc[13-14]. Strong emission peak at 376 nm due to band-to-band transition and green-yellow emission band related to the oxygen vacancy of ZnO NPs is observed [15–17]

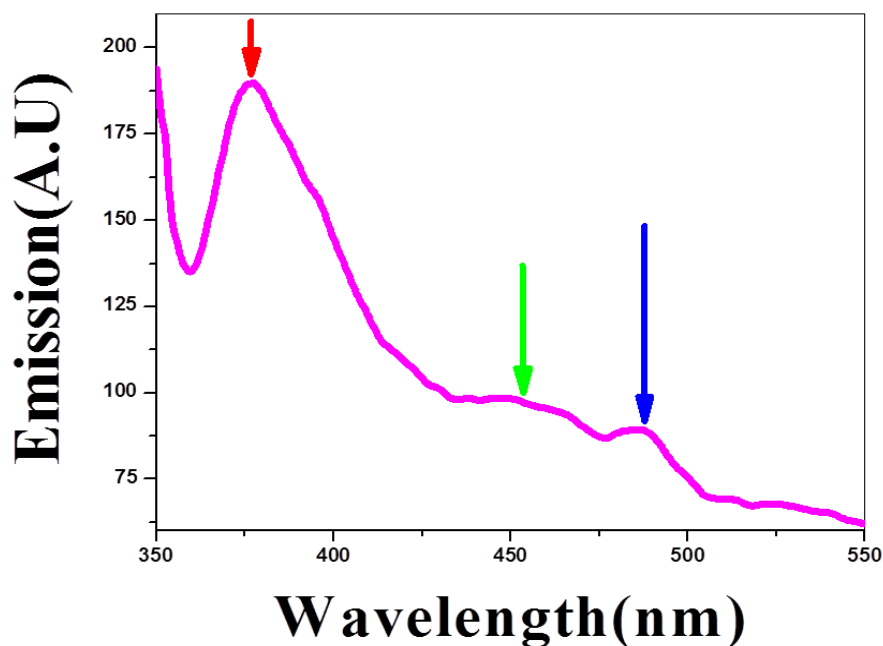


**Figure 3.** Emission spectra of the ZnO NRs

### 3.4. UV-visible spectroscopy and band gap determination

UV-visible spectroscopy was carried out to study further the optical property and determination of the bandgap of the nanorods. The room temperature UV-absorption spectra of the ZnO NRs dispersed in ethanol is shown in figure 4(a). ZnO NRs shows a strong band at 376 nm due to excitonic transition at room temperature [18]. This absorption in the UV region shows one dimensional quantum confinement of carriers [19]. This absorption in the visible range of wavelength implies that there exist more defect energy levels in the synthesized ZnO nanostructures that are due to the specific experimental synthesis conditions. Optical absorption coefficient has been calculated in the Wavelength region 200–900 nm. The bandgap of the as-prepared nanoparticles are determined from the relation [20-23]

$$(\alpha h\nu)^2 = c(h\nu - E_g)$$

where C is a constant.  $E_g$  is the band gap of the material and  $\alpha$  is the absorption coefficient. Figure 1(B) shows the plot of  $(\alpha h\nu)^2$  vs. energy ( $h\nu$ ) and it is used to determine band gap. The band gap of the sample is found to be 3.75 eV (figure 1(B)), which is greater than the bulk ZnO (3.37 eV) [24-25].

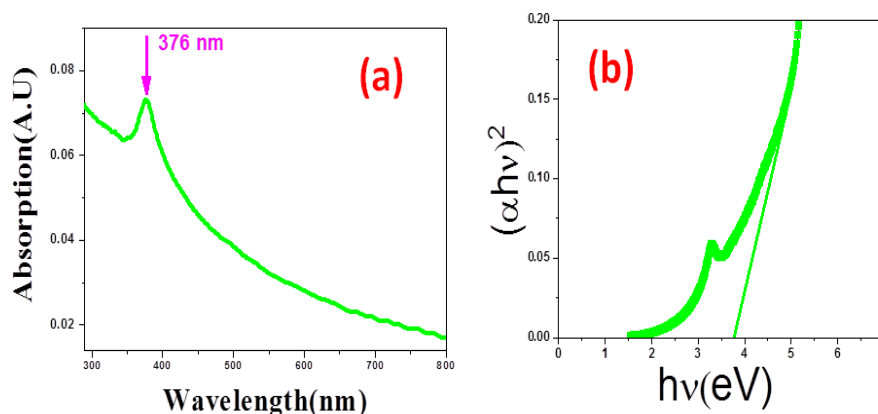


**Figure 4.** (a) UV-VIS absorption spectra of the ZnO nanoparticles, (b) Tauc's plot for the determination of the band gap of the ZnO nanoparticles.

#### 4. Conclusion

We have successfully fabricated ZnO nanorods. The morphology of the ZnO nanorods clearly observed from FESEM images. We have measured Raman spectra of ZnO nanorods and assigned all vibrational modes. The broaden, shift and the asymmetry of the optical phonons have been found for ZnO nanorods. The bandgap of the ZnO NRs is found to be 3.75 eV. Our NRs are good blue emitting material.

#### Acknowledgments

The Authors are grateful to UGC and DST for their constant financial assistance through SAP and FIST program for Department of Physics and Technophysics of Vidyasagar University. The authors are acknowledging to CRF, IIT Kharagpur for different experimental measurement facilities.

#### REFERENCES

1. Z.L.Wang, Zinc oxide nanostructures: growth, properties and applications, *J. Phys. Condens. Matter*, 16 (2004) 829-858.
2. H.M.Xiong, Y.Xu, Q.G.Ren and Y.Y.Xia, Stable Aqueous ZnO@Polymer Core-Shell Nanoparticles with Tunable photoluminescence and Their Application in Cell Imaging, *J. Am. Chem. Soc.*, 130 (2008) 7522-7523.
3. A.K.Bhunia, P.K.Samanta, S.Saha and T.Kamilya, ZnO nanoparticle interaction: Corona formation with associated unfolding, *Applied Physics Letters*, 103 (2013) 1401-1437
4. K.Chung, C.Lee, G.L.Yi, Graphene Layers for Optoelectronic, *Science*, 330 (2010) 655-657.
5. A.K.Bhunia, T.Kamilya and S.Saha, Synthesis, Characterization of ZnO Nanorods and its interaction with Albumin Protein, *Materials Today: Proceedings*, 3 (2016) 592-597.

### Morphological properties and Raman Spectroscopy of ZnO Nanorods

6. S.Radic, P.N.Govindan, R.Chen, E.Salonen, J.M.Brown, P.C.Ke and F.Ding, Effect of fullerene surface chemistry on nanoparticle binding-induced protein misfolding, *Nanoscale*, 6 (2014) 8340-8349.
7. R.P.Wang, G.Xu and P.Jin, Size dependence of electron-phonon coupling in ZnO nanowires, *Phys.Rev. B*, 69 (2004) 1-4.
8. M.Gautam, M.Verma and G.Misra, Structural and optical properties of ZnO nanocrystals, *Journal of Biomedical Nanotechnology*, 7 (2011) 161-162.
9. K.A.Alim, V.A.Fonoberov, M.Shamsa, A.A.Balandin, Micro-Raman investigation of optical phonons in ZnO nanocrystals. *Journal of Applied Physics*, 97 (2005) 1-5.
10. J.G.Ma, Y.C.Liu, R.Mu, J.Y.Zhang, Y.M.Lu, D.Z.Shen and X.W.Fan, Method of control of nitrogen content in ZnO films: Structural and photoluminescence properties, *J. Vac. Sci. Technol. B*, 22 (2004) 94-98.
11. P.K.Samanta and A.K.Bandyopadhyay, Chemical growth of hexagonal zinc oxide nanorods and their optical properties, *Appl Nanosci.*, 2 (2012) 111-117.
12. R.H.Callender, S.S.Sussman, M.Selders and R.K.Chang, Dispersion of Raman cross section in CdS and ZnO over a wide energy range, *Phys. Rev. B*, 7 (1973) 3788-3798.
13. B.X.Lin, Z.X.Fu and Y.B.Jia, Green luminescent center in undoped Zinc Oxide films deposited on silicon substrates, *Appl. Phys. Lett.*, 79 (2001) 943-945.
14. H.Zeng, W.Cai, J.Hu, G.Duan, P.Liu and Y.Li, Violet photoluminescence from shell layer of Zn/ZnO core-shell nanoparticles induced by laser ablation, *Appl. Phys. Lett.*, 88 (2006) 1-3.
15. H.Zeng, G.Duan, Y.Li, S.Yang, X.Xu and W.Cai, Blue luminescence of ZnO nanoparticles based on non-equilibrium process: defect origins and emission controls, *Adv. Funct. Mater*, 20 (2010) 561-572.
16. M.Willander, O.Nur, J.R.Sadaf, M.I.Qadir, S.Zaman, A.Zainelabdin, N.Bano and I. Hussain, Luminescence from zinc oxide nanostructures and polymers and their hybrid devices, *Materials*, 3 (2010) 2643-2667.
17. A.K.Bhunia, T.Kamilya and S.Saha, Optical and structural properties of protein capped ZnO nanoparticles and its antimicrobial activity, *Journal of Advances in Biology & Biotechnology*, 10 (2016) 1-9.
18. Z.Yang, Q.H.Liu, The structural and optical properties of ZnO nanorods via citric acid-assisted annealing route, *Journal of Materials Science*, 43 (2008) 6527-6530.
19. P.K.Samanta, T.Kamilya, A.K.Bhunia, Structural and optical properties of ultra-long ZnO nanorods, *Advanced Science, Engineering and Medicine*, 8 (2016) 128-130.
20. A.K.Bhunia, P.K.Samanta, T.Kamilya and S.Saha, Chemical growth of spherical zinc oxide nanoparticles and their structural, optical properties, *Journal of Physical Sciences*, 20 (2015) 205-212.
21. S.Saha and A.K.Bhunia, Synthesis and characterization of ZnO nanoparticles, *Journal of Physical Sciences*, 19 (2014) 109-114.
22. A.K.Bhunia, T.Kamilya and S.Saha, Temperature dependent and kinetic study of the adsorption of bovine serum albumin to ZnO nanoparticle surfaces, *Chemistry Select*, 1 (2016) 2872-2882.
23. S.Saha and A.K.Bhunia, Synthesis of Fe<sub>2</sub>O<sub>3</sub> nanoparticles and study of its structural, optical properties, *Journal of Physical Sciences*, 17 (2013) 191-195.

A. K. Bhunia, P. K. Jha, D. Rout, S. Saha

24. D.W.Hamby, D.A.Lucca, M.J.Klopfstein and G.Cantwell, Temperature dependent exciton photoluminescence of bulk ZnO, *J. Appl. Phys*, 6 (2003) 3214–3217.
25. Y.Chen, D.M.Bagnall, H.J.Koh, K.T.Park, K.Hiraga, Z.Q.Zhu and T.Yao, Plasma assisted molecular beam epitaxy of ZnO on c-plane sapphire: growth and characterization, *J. Appl. Phys*, 84 (1998) 3912–3918.
26. H.Zeng, G.Duan, Y.Li, S.Yang, X.Xu and W.Cai, Blue luminescence of ZnO nanoparticles based on non-equilibrium processes: defect origin and emission controls, *Adv. Funct. Mater*, 20 (2010) 561-572.